Energy structure of hollow atoms or ions in the bulk of metallic materials

X. M. Tong,[1,*] D. Kato,[1] T. Watanabe,[1] H. Shimizu,[1] C. Yamada,[1,2] and S. Ohtani[1,2]

[1]*''Cold Trapped Ions'' Project, ICORP, JST, Axis 3F, 1-40-2 Fuda Chofu, Tokyo 182-0024, Japan*

[2]*University of Electro-Communication, Chofu, Tokyo 182-0021, Japan*

(Received 17 October 2000; published 13 April 2001)

The local-spin-density functional method, with an optimized effective potential and self-interaction correction, is used to study the energy structure of hollow atoms and ions in the bulk of metallic materials. The energy structure of conduction electrons in the bulk of metallic material is treated by the jellium model. Based on this method, we have studied the x-ray spectra and Auger spectra of N^{q+} hollow atoms and ions in the bulk of Al, as well as in the vacuum. The experimental Auger spectra in the collision of N^{6+} with an insulating surface and conducting surface can be well understood based on our studies. Our calculated x-ray and Auger spectra of hollow atoms or ions in the vacuum and in the bulk of material suggest the need for further systematic experimental investigation.

DOI: 10.1103/PhysRevA.63.052505 PACS number(s): 32.30.Rj, 71.15.Mb, 36.20.Kd

The interaction of highly charged ions (HCI's) with a surface is a subject of increasing interest [1–3]. Basically, three steps are involved in the interaction of HCI's with surfaces: (1) formation of hollow atoms or ions above the surfaces, (2) decay of hollow atoms or ions at or below the surfaces, and (3) total neutralization of hollow atoms or ions in the bulk of materials [1]. The formation of hollow atoms or ions is strongly related to the HCI's impact velocity, incident angle, and other dynamic parameters [4]. In the final neutralization process, hollow atoms or ions emit Auger electrons [5,6] or x rays [7–9]. The emitted x rays provide static information of hollow atoms or ions in the bulk of materials from the energy position, and dynamic information from the spectral intensity. Usually, the Hartree-Fock method is used to study hollow atoms or ions in vacuum [10,11], but the method cannot provide detailed information about the hollow atom or ion in the bulk of materials. To investigate the detailed information of the hollow atom or ion in the bulk of materials, we need to take the conduction-electron screening effect into account. The conduction-electron screening effect was first studied by Zaremba *et al.* [12] using density-functional theory. Recently, Arnau *et al.* [13] used the local-density-functional method to study the energy structure of hollow atoms and ions in the bulk of metallic materials. The advantage of this method is that the total energy of the N-electron system is a functional of the total electron density. Like traditional local-density-functional theory [14], this method contains a spurious self-interaction energy, which should be removed in the exact calculation. To remove the self-interaction energy, we use the local-spin-density-functional method with an optimized effective potential and a self-interaction correction method [15,16]. This method was successfully applied to study the atomic energy structure both in nonrelativistic [16] and relativistic [17] cases. Different from atoms or ions in the vacuum, hollow atoms or ions in the bulk of metallic materials interact with free electrons in the conduction band. Here we treat the conduction electron using the jellium model. The advantages of our method are that (1) we use local-*spin*-density approximation, which allows us to study the spin polarized hollow atoms or ions in the bulk of metallic materials; and (2) we use the optimized effective potential with self-interaction correction for bound electrons, which can completely remove the bound electron self-interaction energy. In our calculations, the Auger and x-ray spectra of N^{q+} hollow atomic ions obtained in the vacuum and near the surface show dramatic differences. Based on our calculated results, the shift and broadening of KLL Auger spectra from N^{6+} collisions on the insulating LiF surface, as compared to those from collisions on the conducting Si surface, can clearly be understood. Meanwhile, the x-ray spectra of a hollow ion in the vacuum can be measured through a microcapillary experiment [18]. Therefore, our theoretical studies will call for a systematic experimental study of the x-ray and Auger spectra of hollow atoms or ions in the vacuum as well as in the bulk of materials.

The energy structure of the conduction electrons in a metallic material can be represented by a jellium model [19]. In the jellium model, the discrete ion cores are replaced by a homogeneous positive background charge, with the charge density equal to the conduction-electron density due to the neutralization requirement. For a given electron density ρ, an effective radius $r_s=(3/(4\pi\rho))^{1/3}$ is defined, and the conduction electrons are filled up to the Fermi energy $\epsilon_F=(1/2r_s^2)(9\pi/4)^{2/3}$. Using density-functional theory with an optimized effective potential and self-interaction correction [16], the total energy $E[\rho]$ of a hollow atom or ion in the bulk of metallic materials can be expressed as (atomic units with $\hbar=m=e=1$ are used throughout unless explicitly stated otherwise)

$$E[\rho]=T_s[\rho]+E_{xc}[\rho_\uparrow,\rho_\downarrow]+V_{ext}[\rho]+J_A[\rho]+E^{SIC}[\rho_b]-T_s[\rho_o]-E_{xc}[\rho_{o_\uparrow},\rho_{o_\downarrow}]-V_{ext}[\rho_o], \quad (1)$$

with

*Email address: tong@hci.jst.go.jp

 ©2001 The American Physical Society

$$V_{ext}[\rho] = -\int \frac{Z}{r}\rho(\mathbf{r})d\mathbf{r},$$

$$J_A[\rho] = \tfrac{1}{2}\int \frac{\rho(\mathbf{r}')\rho(\mathbf{r})}{|\mathbf{r}'-\mathbf{r}|}d\mathbf{r}'d\mathbf{r} - \int \frac{\rho(\mathbf{r}')\rho_o}{|\mathbf{r}'-\mathbf{r}|}d\mathbf{r}'d\mathbf{r} + \tfrac{1}{2}\int \frac{\rho_o\rho_o}{|\mathbf{r}'-\mathbf{r}|}d\mathbf{r}'d\mathbf{r},$$

$$\rho(\mathbf{r}) = \sum_\sigma [\rho_{b\sigma}(\mathbf{r}) + \rho_{o\sigma} + \delta\rho_{c\sigma}(\mathbf{r})] = \rho_b(\mathbf{r}) + \rho_o + \delta\rho_c(\mathbf{r}).$$

Here $T_s[\rho]$ is the noninteracting electron kinetic energy, $E_{xc}[\rho]$ is the exchange-correlation energy, $E^{SIC}[\rho_b]$ is the self-interaction correction for bound electrons [16], and σ is the spin index (spin-up and -down states). ρ_0 is the conduction electron density, ρ_b the bound electron density, and $\delta\rho_c$ the conduction-electron density changes due to the introduction of the hollow atom or ion. The background energy without the hollow atomic ion is subtracted in Eq. (1). The electron wave functions can be obtained by solving the Schrödinger equation as

$$\left[-\frac{\nabla^2}{2} + V_\sigma^{OEP}(\mathbf{r})\right]\psi_{i\sigma}(\mathbf{r}) = \epsilon_{i\sigma}\psi_{i\sigma}(\mathbf{r}), \tag{2}$$

with

$$V_\sigma^{OEP}(\mathbf{r}) = \int \frac{\rho_b(\mathbf{r}') + \delta\rho_c(\mathbf{r}')}{|\mathbf{r}-\mathbf{r}'|}d\mathbf{r}' + \frac{\delta E_{xc}[\rho_\uparrow \cdot \rho_\downarrow]}{\delta\rho_\sigma} + V_\sigma^{SIC}(\mathbf{r}) - \frac{Z}{r} + V_{const},$$

$$\rho_{b\sigma}(\mathbf{r}) = \sum_b \psi_{b\sigma}^*(\mathbf{r})\psi_{b\sigma}(\mathbf{r}), \tag{3}$$

$$\delta\rho_{c\sigma}(\mathbf{r}) = \sum_l \int_0^{k_f} \psi_{l\sigma}^*(r,k)\psi_{l\sigma}(r,k)dk - \rho_{o\sigma}.$$

Note that $r\psi_{l\sigma}(r,k) \to \sqrt{2/\pi}\sin(kr - l\pi/2 + \delta_l\pi)$ when $r \to \infty$; δ_l is the phase shift and k_f is the electron momentum at the Fermi energy.

The bottom of the Fermi energy is chosen as zero of the energy. Equations (2) and (3) can be solved self-consistently. [Note that the self-interaction correction term $V_\sigma^{SIC}(\mathbf{r})$ is constructed in the same way as in Ref. [16].] Since both bond and continuum states are involved in Eq. (2), we use a square grid $[r = r_{max}(i/N)^2, i = 1, N/2]$ in the inner region, which is optimized for bound electrons, and an equal-space grid $[r = r_{max}/4 + 3r_{max}(i - N/2)/(2N), i = N/2 + 1, N]$ in the outer region, which is optimized for conduction electrons. N is the number of grid points used in the calculation. Thus we can describe both the bound and conduction electrons more accurately with limited computational efforts. With the converged optimized effective potential in Eq. (3), we obtain the electron-spin density, total energy, and phase shift for each partial wave.

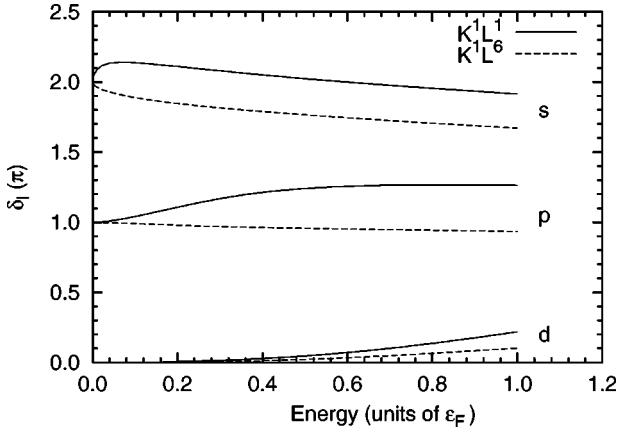

FIG. 1. The phase shifts of the s,p, and d partial waves for K^1L^1 (solid curves) and K^1L^6 (dashed curves) of the N^{q+} hollow atoms or ions in the bulk of Al ($\epsilon_F = 0.4298$ a.u.).

We have calculated the energy structure of the N^{q+} ions in the bulk of Al as well as in the vacuum. r_s of Al metal is 2.07, and the corresponding Fermi energy is 0.430 a.u. The Auger energy or x-ray energy can be obtained from the total-energy difference of the transition between upper and lower states. The numerical convergence was checked by increasing the number of partial waves and the number of radial grid points. The final results presented in this paper were calculated with ten partial waves and 440 radial grid points. In the calculation, we choose $r_{max} = 30r_s$, which is equivalent to including 27 000 conduction electrons in the sphere. The numerical results exhibit almost no change with 15 partial waves and 1000 radial grid points. To study the self-interaction contribution, we have also performed a calculation without self-interaction. Generally speaking, the self-interaction contribution is case dependent. The main self-interaction contribution comes from inner shells. For the present calculation, the self-interaction correction is about 30 eV for the fully filled K shell, and about 20 eV for half-filled K shell.

Figure 1 shows phase shifts for the s, p, and d partial waves in the $1s_\uparrow^1 2p_\downarrow^1$ and $1s_\uparrow^1 2p_\uparrow^3 2p_\downarrow^3$ electron configurations. The phase shifts near zero energy are 2.0, 1.0, and 0.0 for s, p, and d partial waves, respectively. Based on the Levinson theorem [20], we can conclude that two bound states $(1s,2s)$ exist for the s partial wave, one bound state $(2p)$ exists for the p partial wave, and no bound states exist for other higher partial waves. In the vacuum, the number of bound states is infinite, which is quite different from the case in the bulk of metallic materials. For the K^1L^6 configuration, the phase shifts of the s and p partial waves decrease monotonically as the electron energy increases, and the phase shift of the d partial wave increases as the energy increases. For the K^1L^1 configuration, the phase shift of the s partial wave increases first, then decreases as the electron energy increases; the phase shifts of the p and d partial waves increase as the energy increases. From the Friedel sum rule [21], we

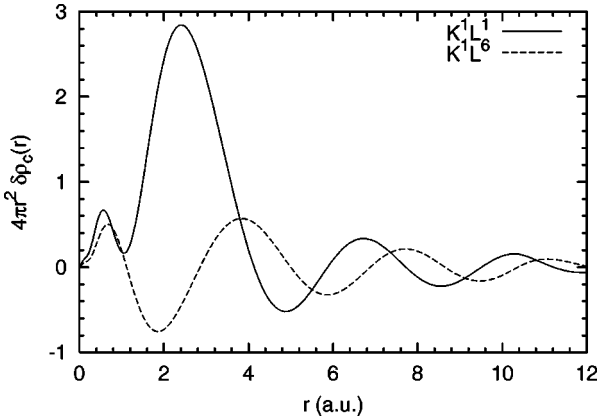

FIG. 2. Conduction electron density changes due to the perturbation of N^{q+} hollow atoms or ions in the bulk of Al.

see that the screening electron comes from the *p* and *d* partial waves for K^1L^1 hollow ions, and the electron in the *s* partial wave is pushed to the outer region. For K^1L^6, the *s* and *p* partial-wave electrons are pushed to the outer region, which is compensated for by the *d* partial-wave electrons. Phase shifts are also very important for studying the stopping power of the low-energy highly charged ions moving in the bulk of metallic materials [22–24].

Figure 2 shows the conduction-electron density changes near the nucleus. Due to the neutralization requirement, we see that more conduction electrons move into the inner region for the less bound-electron case (K^1L^1) and fewer conduction electrons move into the inner region for the most bound-electron case (K^1L^6). The conduction electron density shows the Friedel oscillation [21], as shown in Fig. 2.

Figure 3 shows the calculated x-ray spectra in the bulk of Al and in the vacuum from the total-energy difference between the transition upper and lower states. We see that the emitted x-ray energies from the neutralized hollow atoms (K^1L^6) in the bulk are almost the same as in the vacuum. This can be easily understood, since the conduction-electron screening effect is less important for neutralized hollow atoms. For the most empty hollow ion (K^1L^1), the x-ray energy shifts significantly to lower energies due to the conduction-electron screening effect. In addition to this shift,

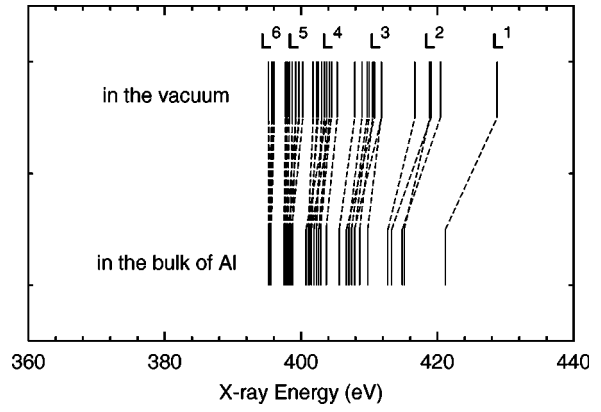

FIG. 3. The x-ray spectra emitted from N^{q+} hollow atoms and ions in the bulk of Al and in vacuum.

TABLE I. The x-ray energies (eV) emitted from the K^1L^2 state of the N^{q+} hollow atoms and ions in the bulk of Al and in vacuum.

	$1s_\uparrow 2s_\uparrow 2p_\downarrow$	$1s_\uparrow 2s_\downarrow 2p_\downarrow$	$1s_\uparrow 2p_\uparrow 2p_\downarrow$	$1s_\uparrow 2p_\downarrow 2p_\downarrow$
Al	414.84	415.12	413.30	412.75
Vacuum	420.34	418.85	419.06	416.70

the energy spectra width within each transition fold (K^1L^n, $n=1,2,\ldots,6$) in the bulk is narrower than that in the vacuum. All such observations can be explained by the conduction-electron screening effect. Due to the conduction-electron screening effect, the total energy of a hollow atom or ion in the bulk of the material is not very sensitive to the total number of electrons and their configuration, as is the case in the vacuum.

A more detailed look at Fig. 3 reveals that the order of energy levels changes from the vacuum to the bulk of Al. To understand the detailed mechanism, we listed the x-ray energy levels for L^2 fold. There are four configurations involved in the transition upper states, $1s_\uparrow 2s_\uparrow 2p_\downarrow$, $1s_\uparrow 2s_\downarrow 2p_\downarrow$, $1s_\uparrow 2p_\uparrow 2p_\downarrow$, and $1s_\uparrow 2p_\downarrow 2p_\downarrow$. In the vacuum, due to spin interaction, the energy level of $2s2p$ is split significantly for spin-up-down and spin-down-down configurations, as listed in Table I. Such energy splitting is of the order of the energy splitting between the $2s2p$ and $2p^2$ configurations. In the bulk of Al, the energy splitting due to different spin configurations is much narrower than that of $2s2p$ and $2p^2$. Therefore, the order of the x-ray energy-level changes. This demonstrates an example in which the local-spin-density approximation is more effective than local-density approximation. Such a spin-polarized effect can be used to identify the x-ray emitted above or below the surface.

In the x-ray transition, only one electron changes its state, and the total number of bound electrons does not change. In the Auger transition, two electrons change their states and one of them leaves the hollow atoms or ions. Therefore, such a transition should be more sensitive to the environment than the x-ray transitions. Since the Auger electron is measured in the vacuum, the Auger electron energy is calculated by the total-energy difference of the transition upper and lower states in the bulk of material, plus the Fermi energy and the work function of the material. Figure 4 shows the calculated Auger spectra of N^{q+} in the bulk of Al and in the vacuum. In the Auger spectra, we cannot find a clear band structure for each L^n fold. The Auger lines in the vacuum cover an energy range of 70 eV, and the Auger lines in the bulk of Al cover an energy range less than 40 eV. Comparing with the experimental energy range of 50 eV [6], we conclude that the Auger electron is neither emitted from the vacuum nor from the bulk of Al. It could be emitted near the surface, and its energy structure is strongly modified by the surface electrons. In the experiment a broadening and an energy shift of the Auger spectra toward the low-energy side has been observed when N^{6+} ions collide with an insulating LiF surface instead of a conducting Si surface. Due to the much lower electron density of an insulating surface, the corresponding Auger spectra resemble the case of electron emission in vacuum much more than an emission resulting from a conducting

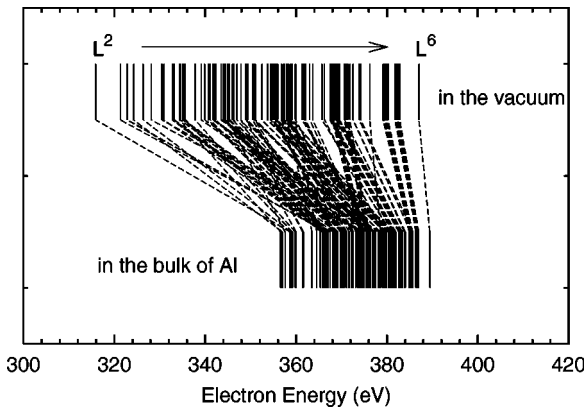

FIG. 4. The Auger spectra emitted from N^{q+} hollow atoms and ions in the bulk of Al and in vacuum.

surface. In our calculation, the Auger spectra exhibit a broader structure in the vacuum than bulk of metallic materials. The energy of Auger electrons emitted in the vacuum is also shifted to the lower-energy side, as shown in Fig. 4. All these features are consistent with the experimental observations [6]. Note that if we take transport effects into account, the Auger spectra will further broaden on the lower-energy side due to the energy loss when the electrons escape from the material. We hope that a systematic experimental investigation both in vacuum and near the surface can be performed in the near future.

To summarize, we have presented a local-spin-density-functional method with an optimized effective potential and self-interaction correction to study the energy structure of highly charged ions in the bulk of metallic material. Using this method, we have studied the x-ray spectra and Auger spectra emitted from the N^{q+} hollow atom or ion in the bulk of Al and in the vacuum. By comparing our calculated Auger spectra with the experimental one [6], we can understand the difference in Auger spectra that results from whether N^{6+} interacts with the insulating surface or the conducting surface. Due to the energy resolution in the experiment, the details of our prediction, namely, the spin-polarized effect, was not observed. We hope the experiments can refine their energy resolution to study the effects.

The authors would like to thank Professor R. Morgenstern and Professor J. G. Snijders for helpful discussions.

[1] J. Burgdörfer, in *Review of Fundamental Processes and Applications of Atoms and Ions*, edited by C. D. Lin (World Scientific, Singapore, 1993), pp. 517–614.
[2] A. Arnau *et al.*, Surf. Sci. Rep. **27**, 113 (1997).
[3] H. Winter and F. Aumayr, J. Phys. B **32**, R39 (1999).
[4] C. Lemell *et al.*, Phys. Rev. A **61**, 012902 (2000).
[5] J. Limburg *et al.*, Phys. Rev. Lett. **73**, 786 (1994).
[6] J. Limburg *et al.*, Phys. Rev. Lett. **75**, 217 (1995).
[7] J. P. Briand *et al.*, Phys. Rev. Lett. **65**, 159 (1990).
[8] J. P. Briand *et al.*, Phys. Rev. A **55**, R2523 (1997).
[9] J. P. Briand *et al.*, Phys. Rev. A **55**, 3947 (1997).
[10] C. P. Bhalla, Phys. Lett. **45A**, 19 (1973).
[11] K. R. Karim, B. Vancleave, and C. P. Bhalla, J. Quant. Spectrosc. Radiat. Transf. **61**, 227 (1999).
[12] E. Zaremba, L. M. Sander, H. B. Shore, and J. H. Rose, J. Phys. F: Met. Phys. **7**, 1763 (1977).
[13] A. Arnau *et al.*, Phys. Rev. A **51**, R3399 (1995).
[14] R. G. Parr and W. T. Yang, *Density-Functional Theory of Atoms and Molecules* (Oxford University Press, New York, 1989).
[15] J. Chen, J. B. Krieger, Y. Li, and G. J. Iafrate, Phys. Rev. A **54**, 3939 (1996).
[16] X. M. Tong and Shih-I. Chu, Phys. Rev. A **55**, 3406 (1997).
[17] X. M. Tong and Shih-I. Chu, Phys. Rev. A **57**, 855 (1998).
[18] S. Ninomiya *et al.*, Phys. Rev. Lett. **78**, 4557 (1997).
[19] A. Zangwill, *Physics at Surface* (Cambridge University Press, Cambridge, 1988).
[20] L. Rosenberg and L. Spruch, Phys. Rev. A **54**, 4985 (1996).
[21] A. Salin, A. Arnau, P. M. Echenique, and E. Zaremba, Phys. Rev. B **59**, 2537 (1999).
[22] I. Nagy, A. Arnau, and P. M. Echenique, Phys. Rev. A **40**, 987 (1989).
[23] W. Zwerger, Phys. Rev. Lett. **79**, 5270 (1997).
[24] J. I. Juaristi *et al.*, Phys. Rev. Lett. **84**, 2124 (2000).